Supplementary Materials

Sub-2 nm PtBi alloy nanoparticles on Bi-N-C single-atom catalyst for selective oxidation of glycerol to 1,3-dihydroxyacetone

Tongyu Tang[1], Hai Zhang[1], Hao-Fan Wang[1], Hongjuan Wang[1], Yonghai Cao[1], Lingyun Zhou[2], Hao Yu[1,*]

[1]School of Chemistry and Chemical Engineering, Guangdong Provincial Key Lab of Green Chemical Product Technology, South China University of Technology, Guangzhou 510641, Guangdong, China.
[2]School of Chemical Engineering, Guizhou Minzu University, Guiyang 550025, Guizhou, China.

[*]**Correspondence to:** Prof. Hao Yu, School of Chemistry and Chemical Engineering, Guangdong Provincial Key Lab of Green Chemical Product Technology, South China University of Technology, 381 Wushan Road, Tianhe District, Guangzhou 510641, Guangdong, China. E-mail: yuhao@scut.edu.cn

A B

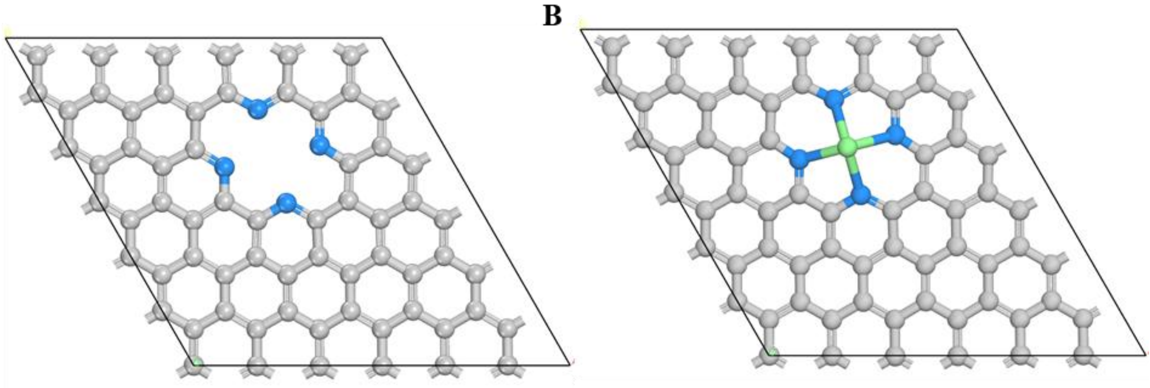

Supplementary Figure 1. The top view of the optimized geometries of the N-doped graphene (A) and Bi modification N-doped graphene (B) models.

A B C D E F G

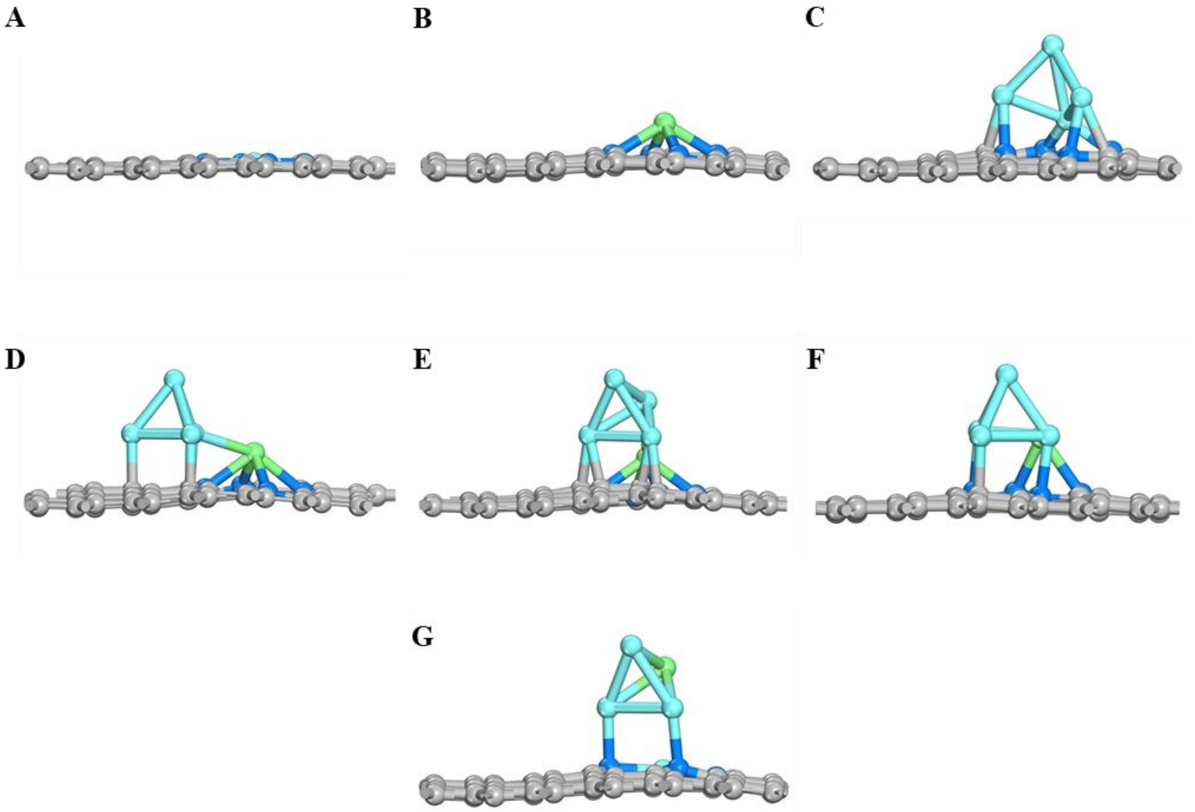

Supplementary Figure 2. The side views of the optimized geometries of (A) a single atomic $Pt-N_4$ site, (B) a single atomic $Bi-N_4$ site, (C) a Pt_4 cluster on N_4 vacancy, (D-G) four geometries of a Pt_4 cluster on a single atomic $Bi-N_4$ site.

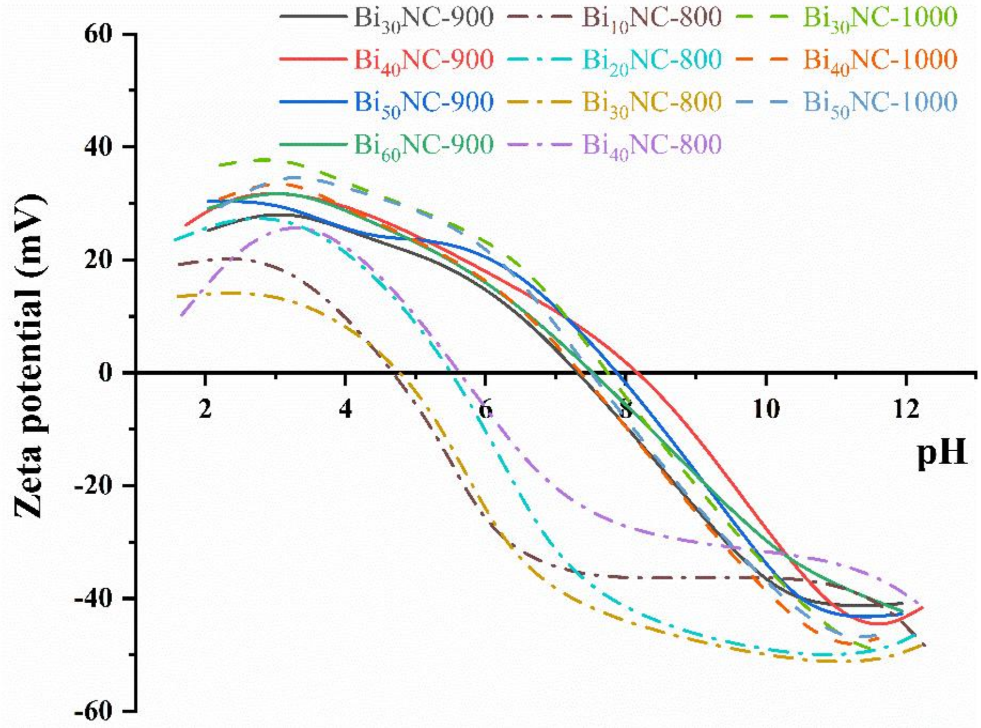

Supplementary Figure 3. Zeta potential measurements of Bi_xNC-*t*.

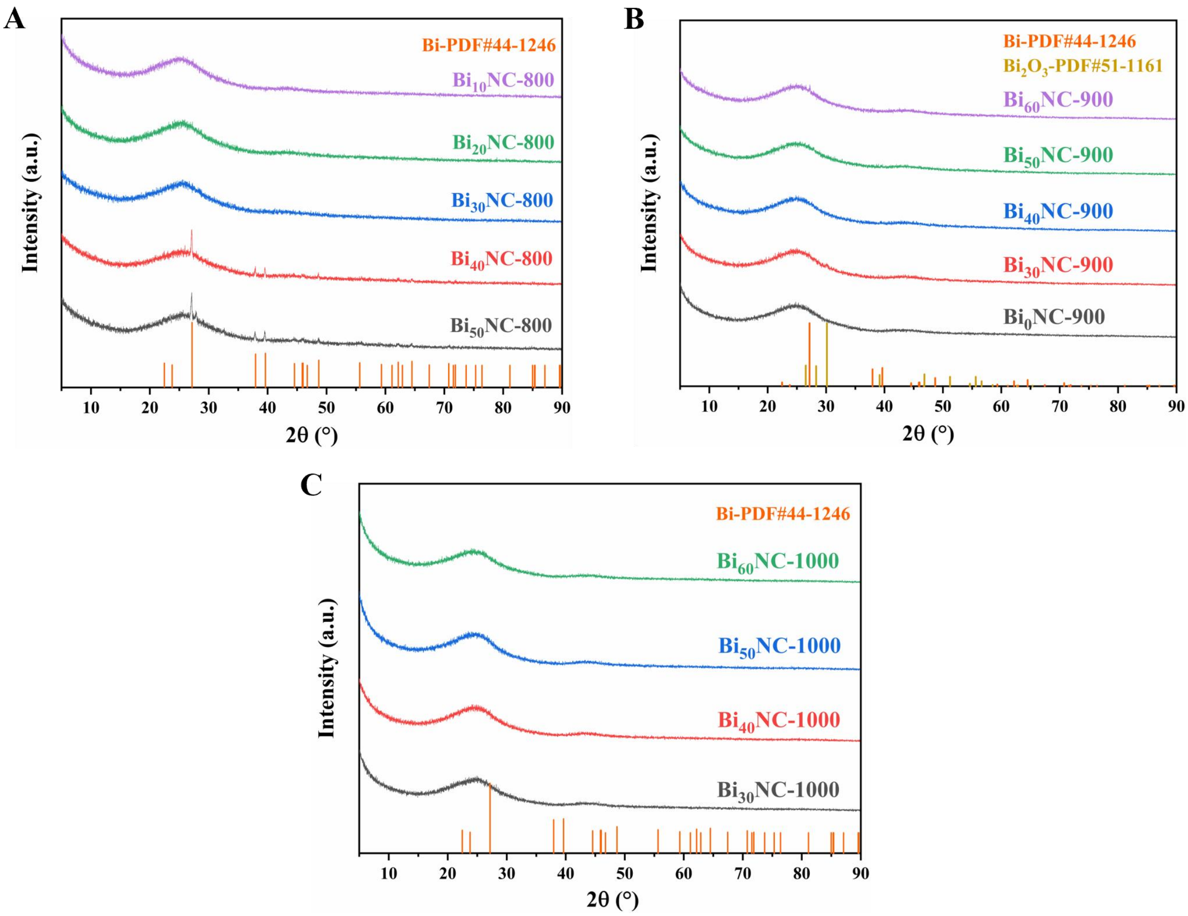

Supplementary Figure 4. XRD patterns of (A) Bi_xNC-800, (B) Bi_xNC-900 and (C) Bi_xNC-1000.

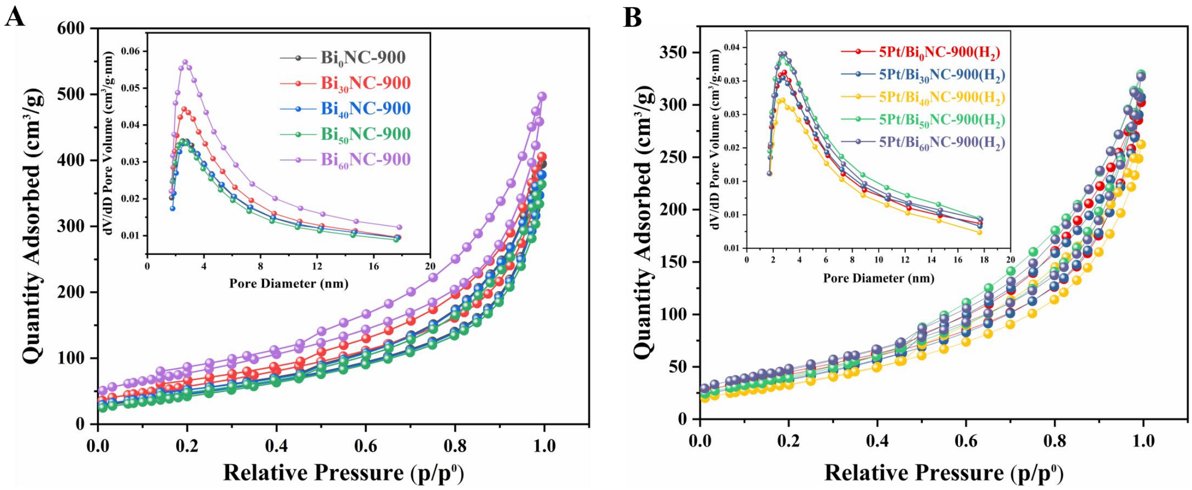

Supplementary Figure 5. N_2 adsorption-desorption isotherms of (A) Bi_xNC-900 and (B) 5Pt/Bi_xNC-900(H_2). The insets show the corresponding pore size distributions.

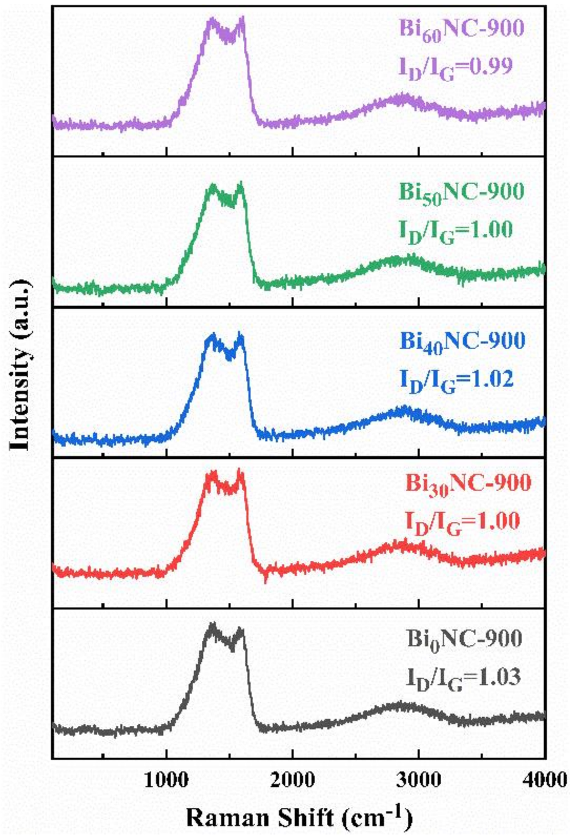

Supplementary Figure 6. Raman spectra of Bi_xNC-900.

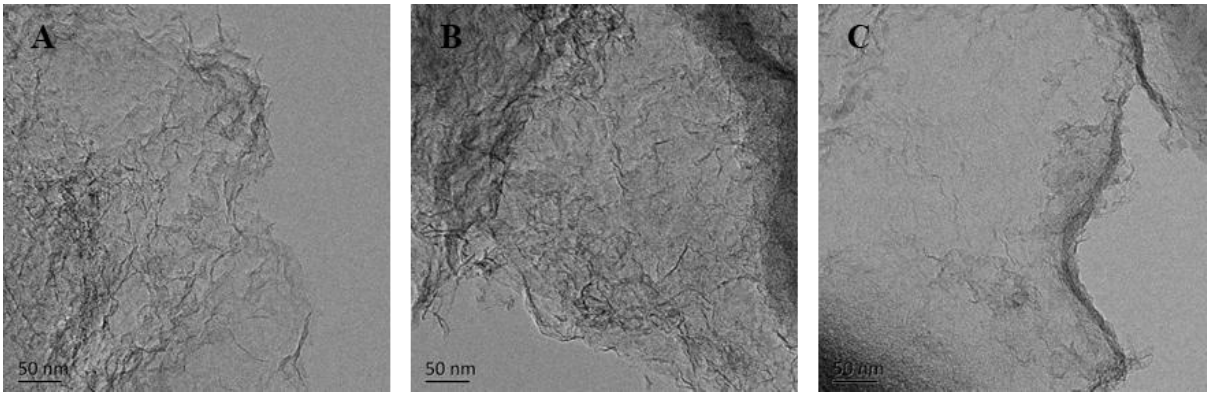

Supplementary Figure 7. TEM images of (A) Bi_{30}NC-900, (B) Bi_{40}NC-900 and (C) Bi_{50}NC-900.

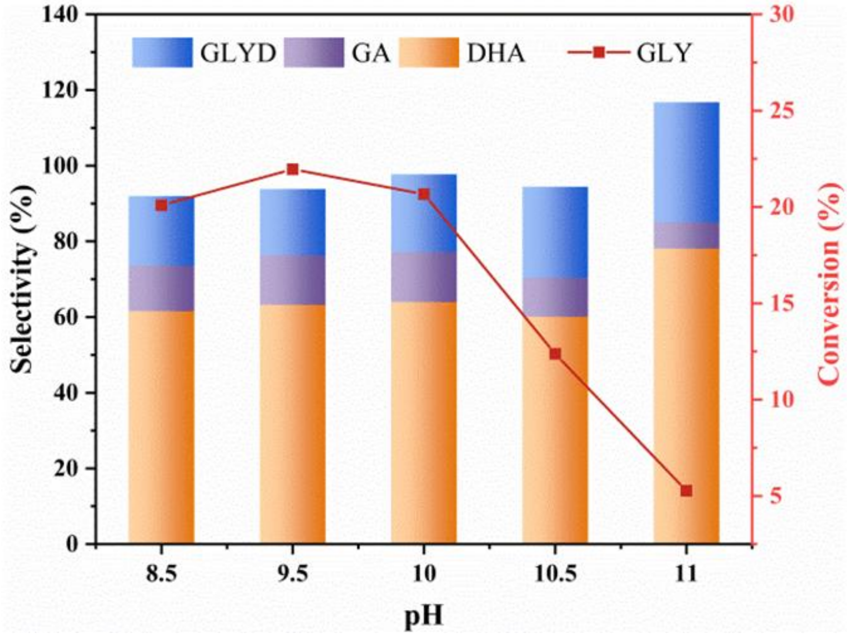

Supplementary Figure 8. The effect of pH during impregnation on the performance of glycerol oxidation over 5Pt/Bi_{50}NC-900(H_2). (Reaction Conditions: 20 g 10 wt.% glycerol solution, 20 mg catalyst, glycerol/Pt molar ratio = 4,300, O_2 flow at 150 Ncm^3/min, 1,200 rpm, 60 ℃, 4 h.)

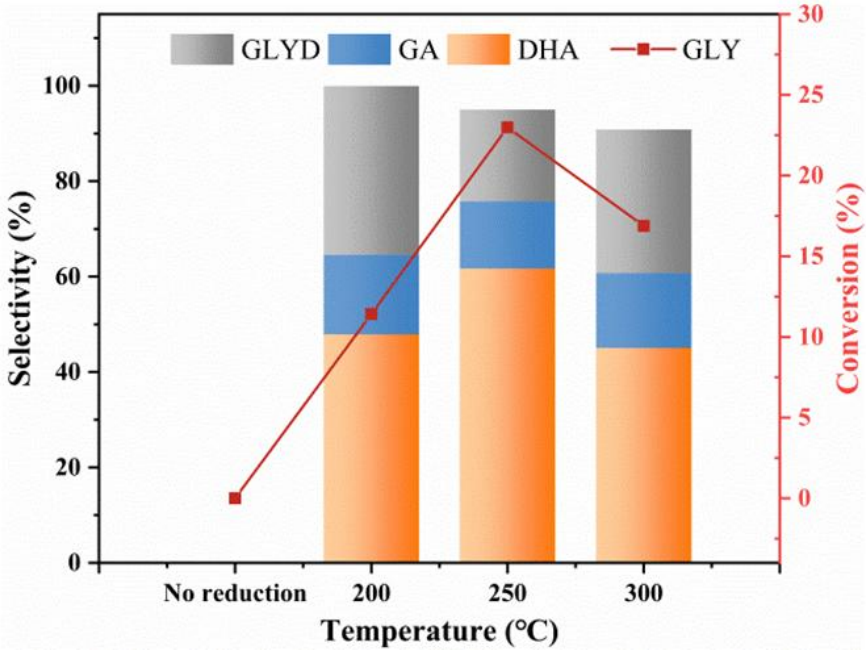

Supplementary Figure 9. The effect of H_2 reduction temperature on the performance of glycerol oxidation over 5Pt/Bi_{50}NC-900(H_2). (Reaction Conditions: 20 g 10 wt.% glycerol solution, 20 mg catalyst, glycerol/Pt molar ratio = 4,300, O_2 flow at 150 Ncm^3/min, 1,200 rpm, 60 °C, 4 h.)

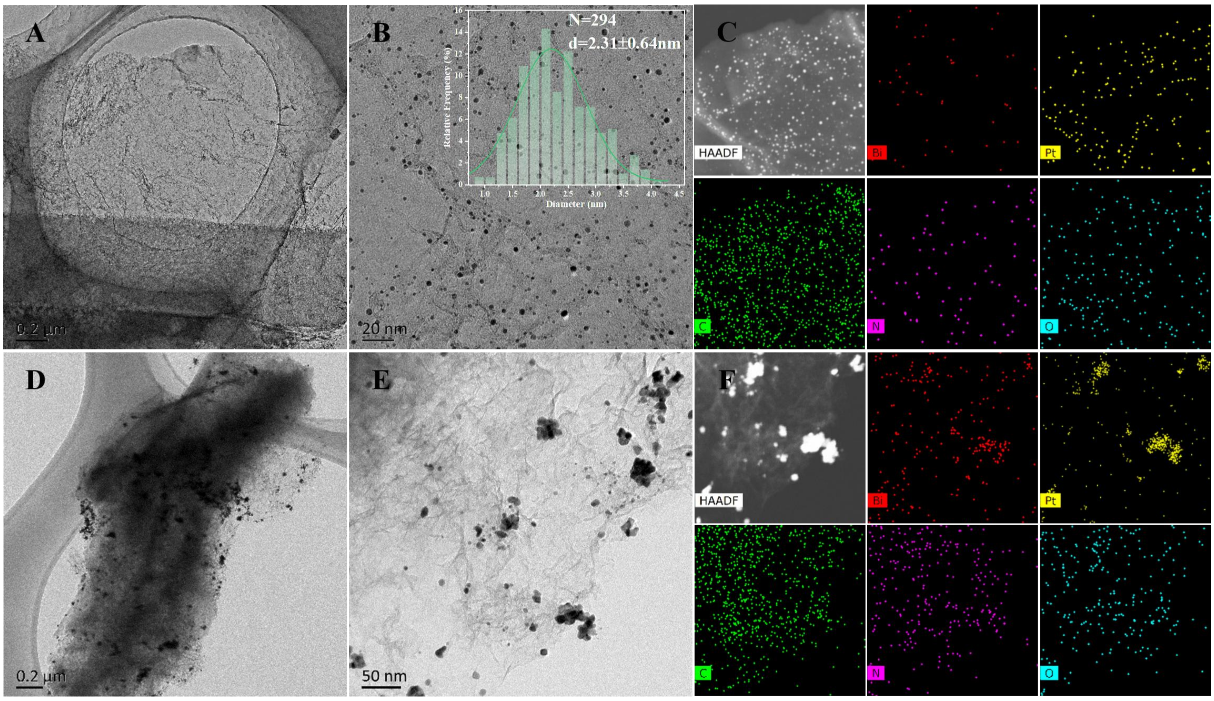

Supplementary Figure 10. (A-B) TEM images and histogram of Pt NP diameters, (C) HAADF-STEM image and associated EDS element maps of 5Pt/Bi_{30}NC-1000(H_2). (D-E) TEM images, (F) HAADF-STEM image and associated EDS element maps of 5Pt/Bi_{30}NC-800(H_2).

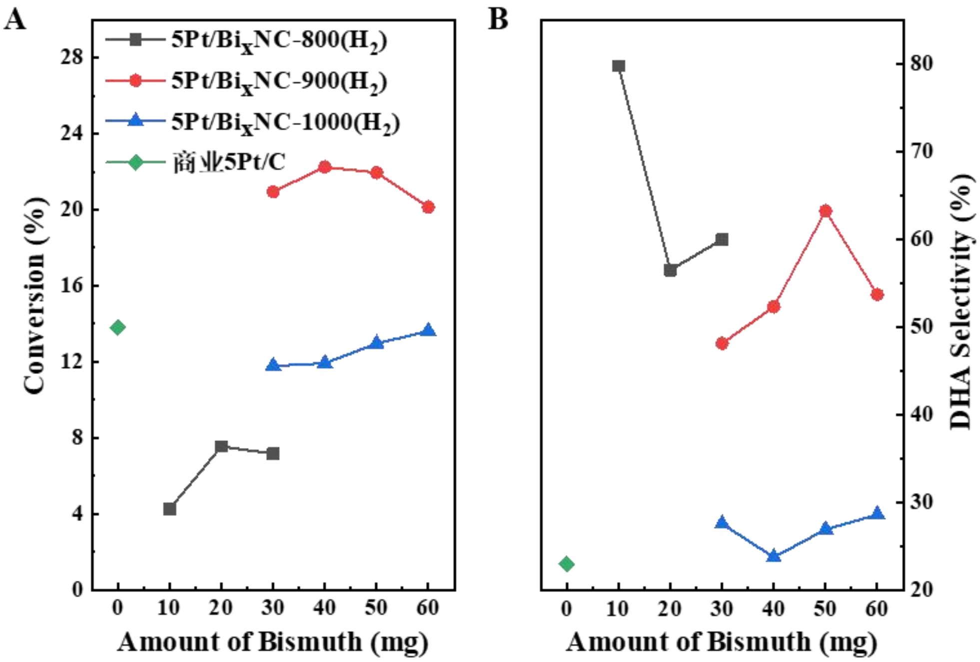

Supplementary Figure 11. Effect of amount of bismuth on (A) glycerol conversion and (B) DHA selectivity over 5Pt/Bi$_x$NC-t(H_2). (Reaction Conditions: 20 g 10 wt.% glycerol solution, 20 mg catalyst, glycerol/Pt molar ratio = 4,300, O_2 flow at 150 Ncm^3/min, 1,200 rpm, 60 °C, 4 h.)

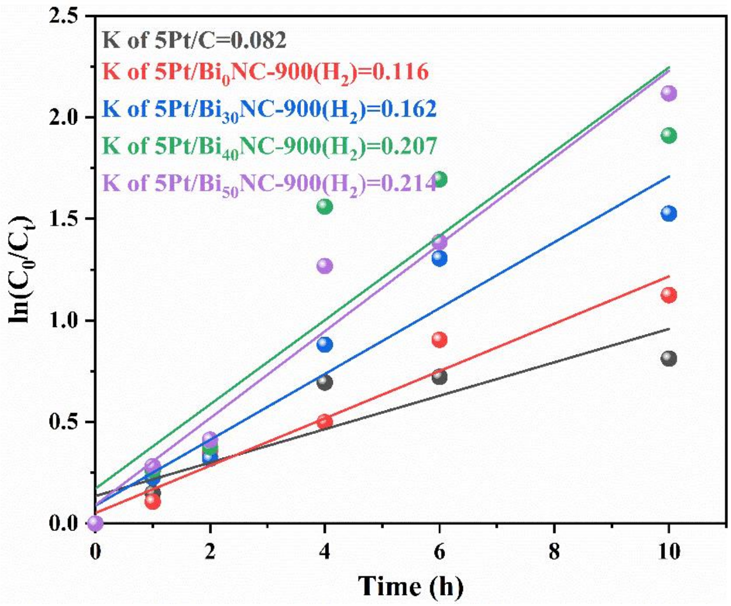

Supplementary Figure 12. Pseudo-first-order reaction rate constant K of 5Pt/Bi_xNC-900(H_2) and commercial 5Pt/C catalysts.

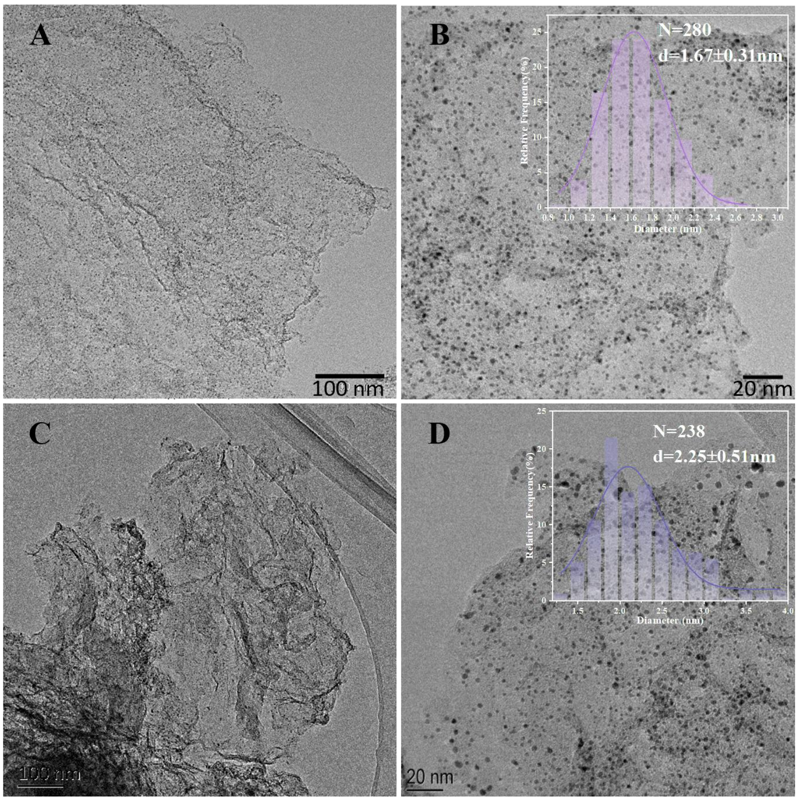

Supplementary Figure 13. (A-B) TEM images of 5Pt/Bi_{50}NC-900(H_2) (before annealing). (C-D) TEM images of 5Pt/Bi_{50}NC-900(H_2) (after four times annealing).

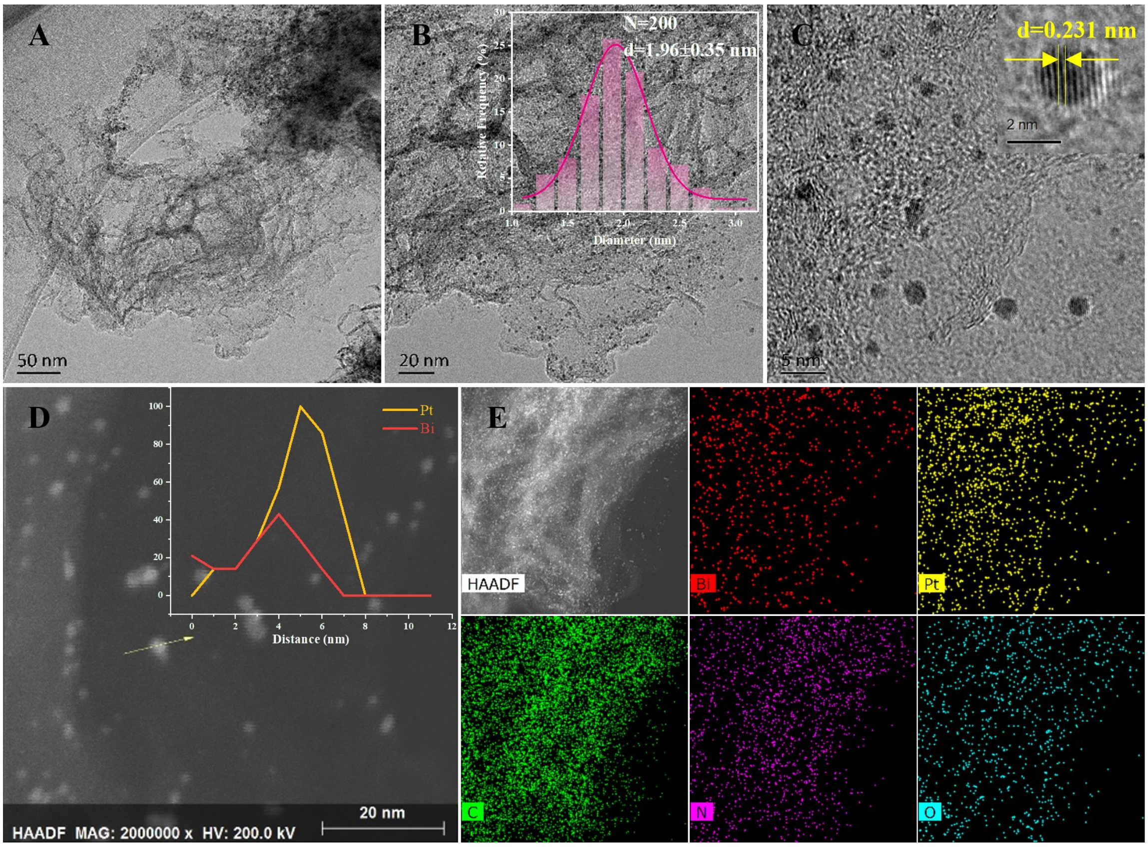

Supplementary Figure 14. (A-C) TEM images and (D) HAADF-STEM image and EDS line scanning of a bright dot, (E) HAADF-STEM image and associated EDS element maps of 2Bi-5Pt/NC-900(H_2).

Supplementary Table 1. Bi contents in Bi_xNC-*t* measured by ICP-OES

Sample	Bi (wt.%)
$Bi_{10}NC$-800	1.66
$Bi_{30}NC$-800	4.37
$Bi_{50}NC$-800	6.77
$Bi_{30}NC$-900	2.56
$Bi_{40}NC$-900	2.79
$Bi_{50}NC$-900	2.51
$Bi_{60}NC$-900	3.68
$Bi_{30}NC$-1000	0.13
$Bi_{40}NC$-1000	0.03
$Bi_{50}NC$-1000	0.14
$Bi_{60}NC$-1000	0.20

Supplementary Table 2. The specific surface areas and pore size distribution of Bi_xNC-900 and 5Pt/Bi_xNC-900(H_2)

Sample	S_{BET} (m^2/g)	Average pore diameter (nm)
Bi_0NC-900	173.9	5.5
$Bi_{30}NC$-900	213.8	5.3
$Bi_{40}NC$-900	171.8	5.6
$Bi_{50}NC$-900	166.3	5.4
$Bi_{60}NC$-900	282.6	5.3
5Pt/Bi_0NC-900(H_2)	160.3	5.6
5Pt/$Bi_{30}NC$-900(H_2)	149.5	5.7
5Pt/$Bi_{40}NC$-900(H_2)	130.8	5.7
5Pt/$Bi_{50}NC$-900(H_2)	161.3	5.7
5Pt/$Bi_{60}NC$-900(H_2)	175.9	5.6

Supplementary Table 3. The representative literature results of PtBi catalysts for the selective oxidation of glycerol to DHA are compared

Authors	Catalysts	d_{TEM} (nm)	D_{Pt} (%)	Reaction conditions	$Sel._{DHA}$ (%)	TOF[b] (h^{-1})	TOF[c] (h^{-1})
This work	$5Pt/Bi_{50}NC-900(H_2)$	1.3	77.0	O_2 150 Ncm^3/min; 60 °C; 1 h; glycerol/Pt = 670	77.4	224.4	166.7
				O_2 150 Ncm^3/min; 60 °C; 4 h; glycerol/Pt = 670	70.2	163.5	121.6
				O_2 150 Ncm^3/min; 60 °C; 6 h; glycerol/Pt = 670	68.4	113.7	84.6
Huang *et al.*[1]	Pt/0.1Bi@NC	2.2	52.2[a]	60 °C; 1 atm air; 1 h; glycerol/Pt = 308	82.3	125.9	65.7
Feng *et al.*[2]	3Pt-0.3Bi/SBA-15	5.2	21.8[a]	1 atm air; 30 °C; 15 h; glycerol/Pt = 65	40.9	12.5	2.7
Xue *et al.*[3]	Pt-7Bi/HT	3.5	32.3[a]	O_2 150 mL/min; 70 °C; 4 h; glycerol/Pt = 424	80.6	54.8	19.3
Xiao *et al.*[4]	Pt-Bi/AC	4.9	22.2	30 psig O_2; 77 °C; 0.8 h; glycerol/Pt = 228	62.8	414.0	91.9
	Pt-Bi/ZSM-5	4.1	27.6		11.7	190.8	52.7
	Pt-Bi/MCM-41	2.2	39.4		46.3	245.4	96.7
	Pt/Bi-MCM-41	2.3	33.9		11.3	168.6	57.2
Ning *et al.*[5]	$PtBi_5/NCNT$	5.4	21.0[a]	O_2 150 Ncm^3/min; 60 °C; 6 h; glycerol/Pt = 482	55.5	116.6	24.5
	Pt/NCNT +Bi/NCNT	3.2	35.4[a]	O_2 150 Ncm^3/min; 60 °C; 6 h; glycerol/Pt = 547	53.3	87.7	31.0
	$Pt/NCNT+Bi(NO_3)_3$	3.7	30.6[a]		64.4	87.4	26.7
Nie *et al.*[6]	Pt-Bi/MWCNTs	2.8	53.4	60 °C; O_2 150 mL/min; 0.2 h; glycerol/Pt = 460.	86.7	500.8	267.4
				60 °C; O_2 150 mL/min; 1.6 h; glycerol/Pt = 460	51.1	276.7	147.8
				60 °C; O_2 150 mL/min; 4.5 h; glycerol/Pt =460	35.6	172.6	92.2
Hu *et al.*[7]	3%Pt-0.6%Bi	4.5	20.3	70 °C, 60 psig, 1 h; glycerol/Pt = 3,251	-	300.0	60.9

[a] D_{TEM} (%) = 5.66/r, where *r* represents the radius of Pt NPs (Å).

[b] $TOF=\frac{n_{0GLY}\times Conv.\%\times Ar_{Pt}}{m_{cat.}\times \omega_{Pt}\times D_{Pt}\times t}$ (The Pt dispersion is considered in the calculation).

[c] $TOF=\frac{n_{0GLY}\times Conv.\%\times Ar_{Pt}}{m_{cat.}\times \omega_{Pt}\times t}$ (The Pt dispersion is not considered in the calculation).

REFERENCES

1. Huang N, Zhang Z, Lu Y, et al. Assembly of platinum nanoparticles and single-atom bismuth for selective oxidation of glycerol. *J Mater Chem A*. 2021;9(45):25576-25584. DOI:10.1039/D1TA07262E

2. Feng S, Yi J, Miura H, Nakatani N, Hada M, Shishido T. Experimental and Theoretical Investigation of the Role of Bismuth in Promoting the Selective Oxidation of Glycerol over Supported Pt-Bi Catalyst under Mild Conditions. *ACS Catal*. 2020;10(11):6071-6083. DOI:10.1021/acscatal.0c00974

3. Xue W, Wang Z, Liang Y, Xu H, Liu L, Dong J. Promoting Role of Bismuth on Hydrotalcite-Supported Platinum Catalysts in Aqueous Phase Oxidation of Glycerol to Dihydroxyacetone. *Catalysts*. 2018;8(1):20. DOI:10.3390/catal8010020

4. Xiao Y, Greeley J, Varma A, Zhao ZJ, Xiao G. An experimental and theoretical study of glycerol oxidation to 1,3-dihydroxyacetone over bimetallic Pt-Bi catalysts. *AIChE Journal*. 2017;63(2):705-715. DOI:10.1002/aic.15418

5. Ning X, Li Y, Yu H, Peng F, Wang H, Yang Y. Promoting role of bismuth and antimony on Pt catalysts for the selective oxidation of glycerol to dihydroxyacetone. *Journal of Catalysis*. 2016;335:95-104. DOI:10.1016/j.jcat.2015.12.020

6. Nie R, Liang D, Shen L, Gao J, Chen P, Hou Z. Selective oxidation of glycerol with oxygen in base-free solution over MWCNTs supported PtSb alloy nanoparticles. *Applied Catalysis B: Environmental*. 2012;127:212-220. DOI:10.1016/j.apcatb.2012.08.026

7. Hu W, Knight D, Lowry B, Varma A. Selective Oxidation of Glycerol to Dihydroxyacetone over Pt-Bi/C Catalyst: Optimization of Catalyst and Reaction Conditions. *Ind Eng Chem Res*. 2010;49(21):10876-10882. DOI:10.1021/ie1005096